MEDICAL SCIENCE MONITOR

LAB/IN VITRO RESEARCH

e-ISSN 1643-3750
© Med Sci Monit, 2018; 24: 1044-1053
DOI: 10.12659/MSM.907739

Received: 2017.10.25
Accepted: 2018.02.01
Published: 2018.02.20

Paeoniflorin Inhibits Receptor Activator for Nuclear Factor κB (RANK) Ligand-Induced Osteoclast Differentiation *In Vitro* and Particle-Induced Osteolysis *In Vivo*

Authors' Contribution:
Study Design A
Data Collection B
Statistical Analysis C
Data Interpretation D
Manuscript Preparation E
Literature Search F
Funds Collection G

ABCD Zhuokai Li*
ABCD De Li*
EF Xiaodong Chen

Department of Orthopedic Surgery, Xinhua Hospital, Shanghai JiaoTong University School of Medicine (SJTUSM), Shanghai, P.R. China

* Contributed equally to this work

Corresponding Author: Xiaodong Chen, e-mail: chenxiaodong@xinhuamed.com.cn

Source of support: This research was supported by the Xinhua Hospital Research Fund (GD201500)

Background: Paeoniflorin (PF), a glucoside isolated from the dried root of Paeonia lactiflora Pall, has been reported to have a number of pharmacological properties, including immunity-regulation, anticancer activities, and neuroprotective effect. However, PF's pharmacological role in bone disorder has been seldom reported. Hence, this study was designed to investigate the effects of PF on osteoclast differentiation and osteolysis diseases.

Material/Methods: The bone marrow macrophages were isolated from C57BL/6 mice and incubated with RANK ligand (RANKL) and various concentrations of PF. After 5 days of incubation, tartrate-resistant acid phosphatase (+) cells and bone resorption pits were counted. Effects of PF on expression of osteoclast-specific protein and gene were investigated via Western blot, q-PCR, and immunofluorescence assay. The osteoprotective effect of PF *in vivo* was evaluated in a calvarial osteolysis model via micro-CT scan and histological stain.

Results: *In vitro*, PF intervention inhibited osteoclast formation and resorption activity. PF also impaired RANKL-induced NF-κB phosphorylation and immigration to the nucleus. PF suppressed osteoclast-marker protein and gene expression. *In vivo*, PF inhibited cobalt-chromium-molybdenum alloy particle-induced osteolysis and reduced osteoclast number in tissue slice.

Conclusions: PF is a potential agent against osteolysis-related diseases caused by excessive osteoclast activity.

MeSH Keywords: Osteoclasts • Paeonia • Prosthesis Failure • Receptor Activator of Nuclear Factor-kappa B

Full-text PDF: https://www.medscimonit.com/abstract/index/idArt/907739

Indexed in: [Current Contents/Clinical Medicine] [SCI Expanded] [ISI Alerting System] [ISI Journals Master List] [Index Medicus/MEDLINE] [EMBASE/Excerpta Medica] [Chemical Abstracts/CAS]

Background

Total hip arthroplasty (THA) is an effective and safe surgery for severe degenerative, post-traumatic, and other end-stage diseases of hip joints. Over 600 000 patients undergo THA every year in the USA, and 0.83% of the U.S population live with an artificial hip joint, which is an estimated 2.5 million individuals [1]. The number of THA surgeries in China is around 250 000 each year (unofficial statistics). According to reported data, aseptic loosening is the primary reason for THA failures. Osteolysis bone defect, longer operative time, and excessive blood loss during revision surgery lead to greater surgical challenge and medical cost. Hence, extending the life of artificial joints and avoiding revision surgery are important.

The exact mechanism of aseptic loosening remains unclear, but wear particle is generally considered to be the triggering factor. Wear particles (like cobalt-chromium-molybdenum alloy), are continuously generated from bearing surfaces in continuous surface movements. Phagocytes endocytose the particles and release a cascade of pro-inflammatory cytokines into the tissues surrounding the implants, including tumor necrosis factor alpha (TNF-α), interleukin (IL)-1β, and IL-6 [2,3]. These cytokines along with wear particles stimulate osteoclast differentiation directly or indirectly [4–6]. Eventually, enhanced osteoclast activity leads to periprosthetic osteolysis [7].

Paeoniflorin (PF) has been used frequently as a neuroprotective and anti-inflammatory agent [8–10]. Studies have reported that PF protects against brain injury and lipopolysaccharide-induced acute lung injury by inhibiting inflammatory responses via inhibiting NF-κB [11,12]. Considering that NF-κB plays a central role in osteoclast formation and wear particle-induced osteolysis [13–15], we hypothesized that PF has a regulatory effect on osteoclast formation and wear particle-induced osteolysis. Therefore, we designed the following experiments to investigate the pharmacological action of PF both *in vitro* and *in vivo*.

Material and Methods

Reagents and CoCrMo particles

Paeoniflorin agent (lot no. 75603) and tartrate-resistant acid phosphatase (TRAP) staining kits were purchased from Sigma-Aldrich (St. Louis, MO, USA). Recombinant murine RANKL and murine colony stimulating factor (M-CSF) were purchased from PeproTech (Rocky Hill, NJ, USA). All antibodies used in this research were purchased from the Cell Signaling Technology (Boston, MA, USA). The CoCrMo particles were purchased from Zimmer Medical Group (Warsaw, IN, USA) with an average diameter of 100 nm, which is similar to clinical wear particle size. Particles were washed in a 70% ethanol solution to remove bound endotoxin and determined to be endotoxin-free using the Limulus assay (Endosafe, Charles Rivers, Charlestown, SC, USA). The particles were suspended in sterile phosphate-buffered saline (PBS) at a concentration of 0.1 mg/μL for further experiments. Scanning electron microscopy (SEM) was carried out to characterize the size of particles (S3400I, Hitachi, Japan).

Bone marrow macrophage (BMM) preparation and cell culture

Procedures involving animals and their care were conducted in conformity with NIH guidelines (NIH Pub. No. 85-23, revised 1996) and were approved by the Ethics Committee of Xinhua Hospital Affiliated to Shanghai Jiao Tong University School of Medicine (approval no. XHEC-F-2017-010).

BMMs were prepared as detailed in a previously published paper with some modifications [16]. In brief, BMMs were collected from the tibias and femurs of two 6-week-old C57BL mice by flushing the marrow space with alpha-modified minimum essential medium (α-MEM). The bone marrow cells were incubated in α-MEM with 10% fetal bovine serum (FBS) overnight (>16 h). Non-adherent cells were collected and seeded in a new 10-cm culture dish containing α-MEM with 10% FBS, penicillin (100 U/mL), streptomycin (100 μg/mL), and M-CSF (20 ng/mL). After a 3-day incubation, the non-adherent cells were removed and the adherent cells were washed with medium and harvested using a trypsin-EDTA solution (0.25%) for further experiments.

Cell counting kit 8 (CCK-8)

BMMs were seeded onto 96-well plates at a concentration of 2×10^4 cells/well and then incubated with PF (0, 5, 20, 50, 100, 150, 200 μmol/L) for 24 h. We added 10 mL of CCK-8 to each well and the plate were incubated at 37°C for 2 h. The optical density (OD) was measured using an ELX800 absorbance microplate reader (Bio-Tek; USA) at 450 nm. Cell viability was calculated relative to the control ([experimental group OD-blank OD]/[control group OD-blank OD]).

In vitro osteoclast differentiation and TRAP staining

BMMs were seeded onto 96-well plates at a concentration of 2×10^4 cells/well. Medium containing PF (5, 20, 50, or 100 μM) was added to the wells along with RANKL (50 ng/mL) and M-CSF (30 ng/mL). BMMs were fixed and TRAP stained per the manufacturer's instructions (Sigma-Aldrich) after incubating for 5 days. TRAP-positive osteoclasts were counted on 4 randomly selected fields of view for each well. The experiment was repeated 3 times.

Indexed in: [Current Contents/Clinical Medicine] [SCI Expanded] [ISI Alerting System] [ISI Journals Master List] [Index Medicus/MEDLINE] [EMBASE/Excerpta Medica] [Chemical Abstracts/CAS]

Resorption pit assay

As for bone resorption assay, BMMs were seeded onto Coring 96-well plates (lot no. 3988) at a density of 2×10^4 cells/well with M-CSF (30 ng/mL) and RANKL (50 ng/mL). On day 5, the medium was aspirated from the wells and 100 µL of 10% bleach solution was added. Cells were incubated with the bleach solution for 5 min at room temperature. The wells were washed twice with PBS and allowed to dry at room temperature for 3–5 h. Resorption pits were counted on 4 randomly selected fields of view for each well. The pit resorption areas were measured using Image Pro Plus 6.0 and the percentage of resorption area was measured.

Quantitative polymerase chain reaction (q-PCR)

Expression of osteoclast-related gene was measured by quantitative polymerase chain reaction-PCR. 10^6 BMM cells were seeded into each well of 6-well plates. The cells were treated with complete medium containing a-MEM, 10% FBS, M-CSF (30 ng/mL), and RANKL (50 ng/mL), with or without PF (20, 100 µM). Total RNA was extracted with Trizol solution after 24-h incubation. Reverse transcription PCR was executed using reverse transcriptase (Takara, Ōtsu, Japan). q-PCR was carried out with 200 ng cDNA, the PrimeScript RT-PCR Kit (Takara, Ōtsu, Japan) in 96-well plates, and an ABI 7500 Sequence Detection System (Applied Biosystems, Foster City, USA) per the manufacturer's instructions. β-*Actin* was used as the housekeeping gene, and the experiment was repeated 3 times. The following primer sets were used (5'-3'): mouse β-*actin*: forward, TCTGCTGGAAGGTGGACAGT and reverse, CCTCTATGCCAACACAGTGC;
mouse *NFATc1*: forward, CCGTTGCTTCCAGAAAATAACA and reverse, TGTGGGATGTGAACTCGGAA; mouse *TRAP*: forward, CTGGA GTGCACGATGCCAGCGACA and reverse, TCCGTGCTCGGCG ATGGACCAGA;
mouse *Cathepsin K*: forward, CTTCCAATACGTGCAGCAGA and reverse, TCTTCAGGGCTTTCTCGTTC; mouse *c-Fos*: forward, CCAGTC AAGAGCATCAGCAA and reverse, AAGTAGTGCAGCCCGGAGTA.

Western blotting in BMM cells

BMM cells were seeded at 5×10^5 cells/well into 6-well plates and treated with or without PF and RANKL (100 ng/mL) for the indicated duration. BMM cells were lysed with radioimmunoprecipitation assay (RIPA) buffer (Beyotime, Shanghai, China), and proteins were extracted per the manufacturer's instructions. Protein concentrations were determined using a bicinchoninic acid (BCA) assay. Each sample (30 µg protein) was fractionated on an 8% sodium dodecyl sulfate polyacrylamide gel electrophoresis (SDS-PAGE) gel and transferred to polyvinylidene difluoride (PVDF) membranes. The membranes were then blocked in non-fat milk for 1 h and incubated with the indicated primary antibodies (1: 1000 dilution) at 4°C overnight. Subsequently, the membranes were incubated with an appropriate secondary antibody (1: 1000 dilution) for 1 h at 20°C. The proteins were detected using a horseradish peroxidase (HRP) solution. The grey values were analyzed by Image J software, normalized by β-actin. Experiments were repeated 3 times.

BMM immunofluorescence

BMMs were seeded onto 96-well plates and allowed to adhere and then treated with or without PF (100 µM) for 1 h and stimulated with RANKL (100 ng/mL) for 15 min. Cells were fixed with 4% paraformaldehyde and permeabilized with 0.5% Triton X-100. The BMMs were then sequentially incubated with primary antibodies against NF-κB (p65) protein and secondary fluorescein isothiocyanate-conjugated antibodies. For reference, cells were stained with 4',6-diamidino-2-phenylindole (DAPI); tubulin proteins were also stained. Activation of NF-κB signaling was determined by measuring translocation of p65 into the nucleus.

Murine calvarial osteolysis model

We assigned the 20 C57BL mice (6 weeks old) to 1 of 4 experimental groups: PBS control group (group 1), CoCrMo particle group (group 2), CoCrMo particles with 20 mg/kg/day PF group (group 3), and CoCrMo particles with 100 mg/kg/day PF group (group 4). The mice were anesthetized with an intraperitoneal injection containing 0.2 mL chloral hydrate (5%). A 1.5-cm incision was made longitudinally over the craniums exposing the junction zone of the frontal and parietal bones. The periosteum was gently erased. In group 1, the incision was closed without any further intervention using 3-0 un-absorbable sutures. In groups 2–4, the incision was closed as described for group 1 and then a 3-mg CoCrMo particle suspension (30 µL) was injected into the periosteum-removed area using a microsyringe. In groups 3–4, the mice received an intraperitoneal injection of 20 mg/kg/day or 100 mg/kg/day PF (dissolved in PBS) until Day 7; groups 1–2 were injected with an equal volume of PBS until Day 7. All mice were fed in an aseptic environment with free access to food and water. No adverse effects or mortality occurred during the study. Seven days after surgery, the mice were sacrificed by an overdose injection of sodium pentobarbital solution, and the craniums were harvested for micro-computerized tomography (µ-CT) and histological analyses.

Micro-CT scanning and histological analysis

Paraformaldehyde-fixed craniums were scanned with a high-resolution CT scanner (SkyScan 1176; SkyScan, Kontich, Belgium) using a resolution of 18 mm and operating at a source voltage

Indexed in: [Current Contents/Clinical Medicine] [SCI Expanded] [ISI Alerting System] [ISI Journals Master List] [Index Medicus/MEDLINE] [EMBASE/Excerpta Medica] [Chemical Abstracts/CAS]

of 80 kV and 100 mA. After scanning, three-dimensional images were reconstructed using the software provided with the μ-CT system; a square area of interest (AOI) around the midline suture was chosen for further qualitative and quantitative analysis. The ratio of bone volume to tissue volume (BV/TV) and the bone mineral density (BMD, mg/mm^3) from the AOI were obtained using the μ-CT software provided with the system. The percentage of porosity in AOI was analyzed using Image Pro Plus 6.0 software.

For histology, the craniums were fixed in 4% paraformaldehyde for 24 h and then decalcified in ethylenediaminetetraacetic acid (EDTA, 10%) for 1 week. After the tissue slices were prepared, hematoxylin and eosin (H&E) staining and TRAP staining were performed based on standard procedures. TRAP-positive osteoclasts on each bone surface were counted via Image Pro Plus 6.0 as previously described [17,18].

Statistical analyses

All statistical analyses were performed with SPSS 22.0 software. The *t* test was performed when there were 2 groups of data. One-way ANOVA was used when the data were more than 3 groups. Student-Newman-Keuls (SNK) was performed to measure significance between each group when the data were more than 3 groups. And $p<0.05$ was considered to indicate a statistically significant difference.

Results

Effects of PF on cytotoxicity, osteoclast formation, and resorption activity

At concentrations below 200 μM, PF had no significant impact on BMM survival (Figure 1 A). The TRAP stain results showed that PF remarkably inhibited RANKL-induced mature osteoclast formation in a dose-dependent manner (Figure 1B, 1C), with 196.33±15.82, 150.66±16.04, 118.67±15.04, 96.33±7.37, and 22.33±8.73 osteoclasts/well, respectively.

Afterwards, we measured the impact of PF on osteoclast resorption capacity via Corning osteo assay plate. BMM cells were stimulated with RANKL + M-CSF to induce the differentiation of mature osteoclasts with bone resorption capacity. The ratio of resorption area to whole area in each sight was measured. And the result showed that PF inhibited the size resorption area in each well in a dose-dependent manner (Figure 1D) with 51.92±3.69%, 37.93±2.60%, 28.67±2.87%, 21.56±3.29%, and 5.78±2.43% at 0, 5, 20, 50, and 100 μM concentrations, respectively.

These results collectively demonstrate that paeoniflorin inhibited both the formation and bone resorption properties of osteoclasts.

PF inhibits NF-κB signaling pathway

As its name indicates, NF-κB is an essential downstream protein for RANKL-induced osteoclast formation [19]. Western blot results showed that RANKL lead to phosphorylation of p65, which was in accordance with reported results (Figure 2A). Further, PF substantially reduced phosphorylation of p65, suggesting that PF inhibited osteoclast formation by blocking NF-κB activation (Figure 2B). Meanwhile, PF had little influence on phosphorylation of mitogen-activated protein kinase (MAPK) family proteins, which can also regulate osteoclast differentiation [20,21].

To confirm the influence of PF on NF-κB signaling, we performed immunofluorescent staining of the NF-κB p65 subunit with or without PF (100 μM) treatment. RANKL treatment resulted in translocation of the p65 protein to the nucleus in BMMs. Moreover, PF blocked RANKL-induced translocation of p65 to cell nucleus (Figure 2C), which confirmed that PF impaired osteoclast formation as a NF-κB inhibitor. Overall, these results suggest that PF participates in the regulation of RANKL-induced NF-κB activation, and can thus contribute to the inhibition of osteoclast formation.

NFATc1 and c-Fos are 2 important nuclear transcriptional factors regulating osteoclast differentiation [22,23]. To determine whether PF regulates the expression of NFATc1, we next assessed the effects of PF on RANKL-induced NFATc1 and c-Fos expression. As shown in Figure 2D, protein levels of NFATc1 and c-Fos increased when BMMs were exposed to RANKL, and PF treatment inhibited the increase of NFATc1 and c-Fos expression. These results suggest that PF inhibits osteoclast formation via regulating NFATc1 and c-Fos expression.

PF inhibits osteoclast-related genes expression

Afterwards, we used q-PCR to measure the effects of PF (20 and 100 μM) on key osteoclast-gene expression (Figure 3). *NFATc1* is a master switch for regulating terminal differentiation of osteoclasts functioning downstream of RANKL/RANK [24–26]. *c-Fos* is a member of the Fos family of genes that with Jun proteins form the AP-1 family of heterodimeric transcription factors. AP-1 acts as an essential switch for osteoclast differentiation from the progenitor, and osteoclasts do not form in its absence. AP-1 also regulates the expression of NFATc1 at the initial stage of osteoclast differentiation [27]. PF treatment remarkably inhibited the key genes, *NFATc1* and *c-Fos*. PF also remarkably inhibited absorbing-related gene expression, *TRAP* and *Cathepsin K*. Further, 100 μM PF showed more inhibiting effects than 20 μM.

Indexed in: [Current Contents/Clinical Medicine] [SCI Expanded] [ISI Alerting System] [ISI Journals Master List] [Index Medicus/MEDLINE] [EMBASE/Excerpta Medica] [Chemical Abstracts/CAS]

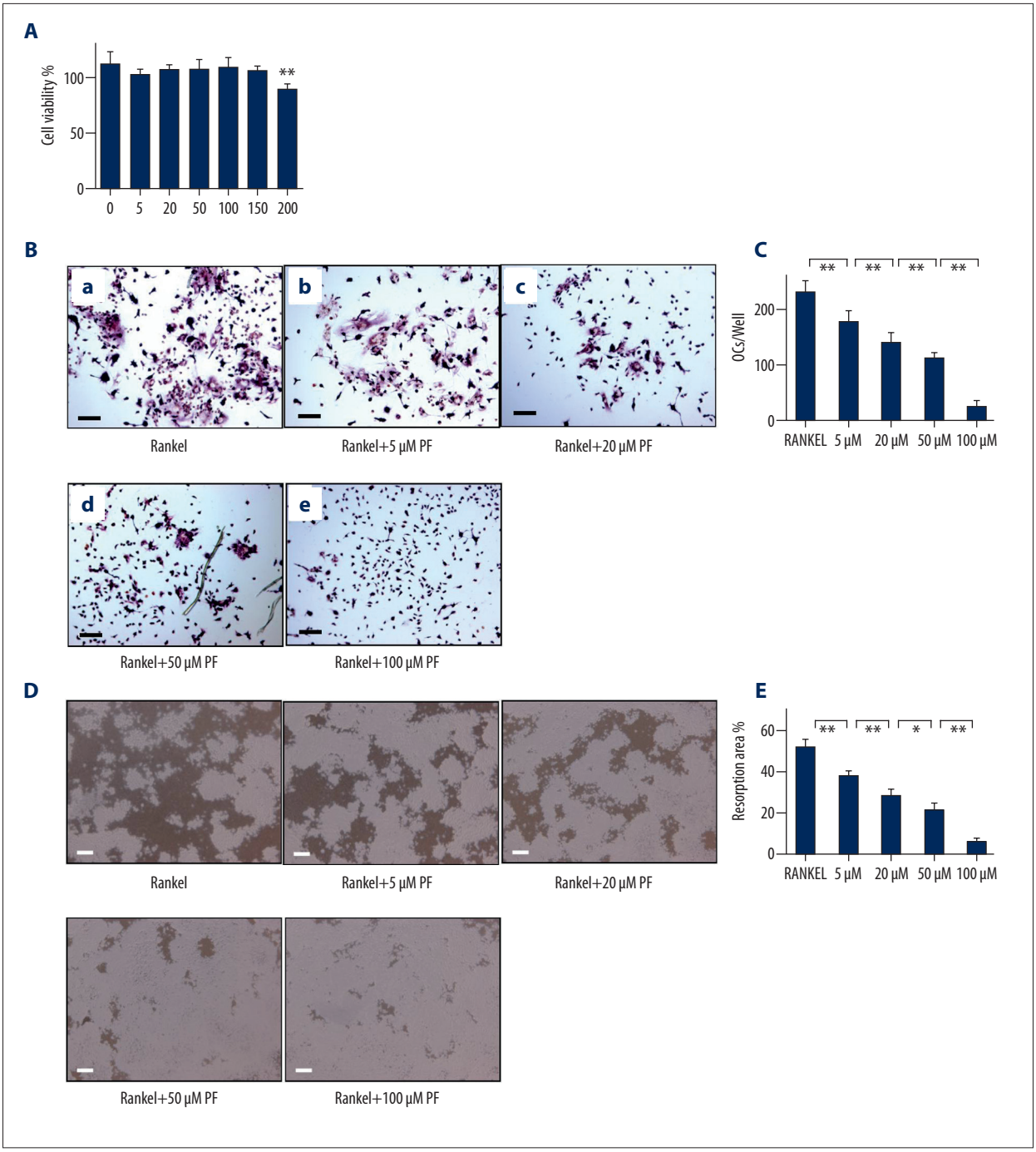

Figure 1. Paeoniflorin inhibits RANKL-induced osteoclast formation bone resorption. (**A**) Bone marrow macrophages (BMMs) were incubated with various concentrations of PF for 24 h. PF toxicity was measured using the cell counting kit 8 (CCK-8) assay. OD, optical density; (**B, C**) BMMs were incubated with RANKL (50 ng/mL) + murine colony stimulating factor (M-CSF) (30 ng/mL) in a 96-well plate along with various concentrations of paeoniflorin for 5 days. Tartrate-resistant acid phosphatase (TRAP)-positive cells in each well were counted; (**D, E**) BMMs were seeded in the osteo assay plate, cultured in the presence of RANKL (50 ng/ml) + M-CSF (30 ng/ml) and with the indicated concentration of PF. After 5 days of incubation, pit resorption areas were measured. All experiments were repeated 3 times. One-way ANOVA and Student-Newman-Keuls (SNK) tests were performed to measure significances between each group. * $p<0.05$, ** $p<0.01$, scale bar=100 μm.

Indexed in: [Current Contents/Clinical Medicine] [SCI Expanded] [ISI Alerting System] [ISI Journals Master List] [Index Medicus/MEDLINE] [EMBASE/Excerpta Medica] [Chemical Abstracts/CAS]

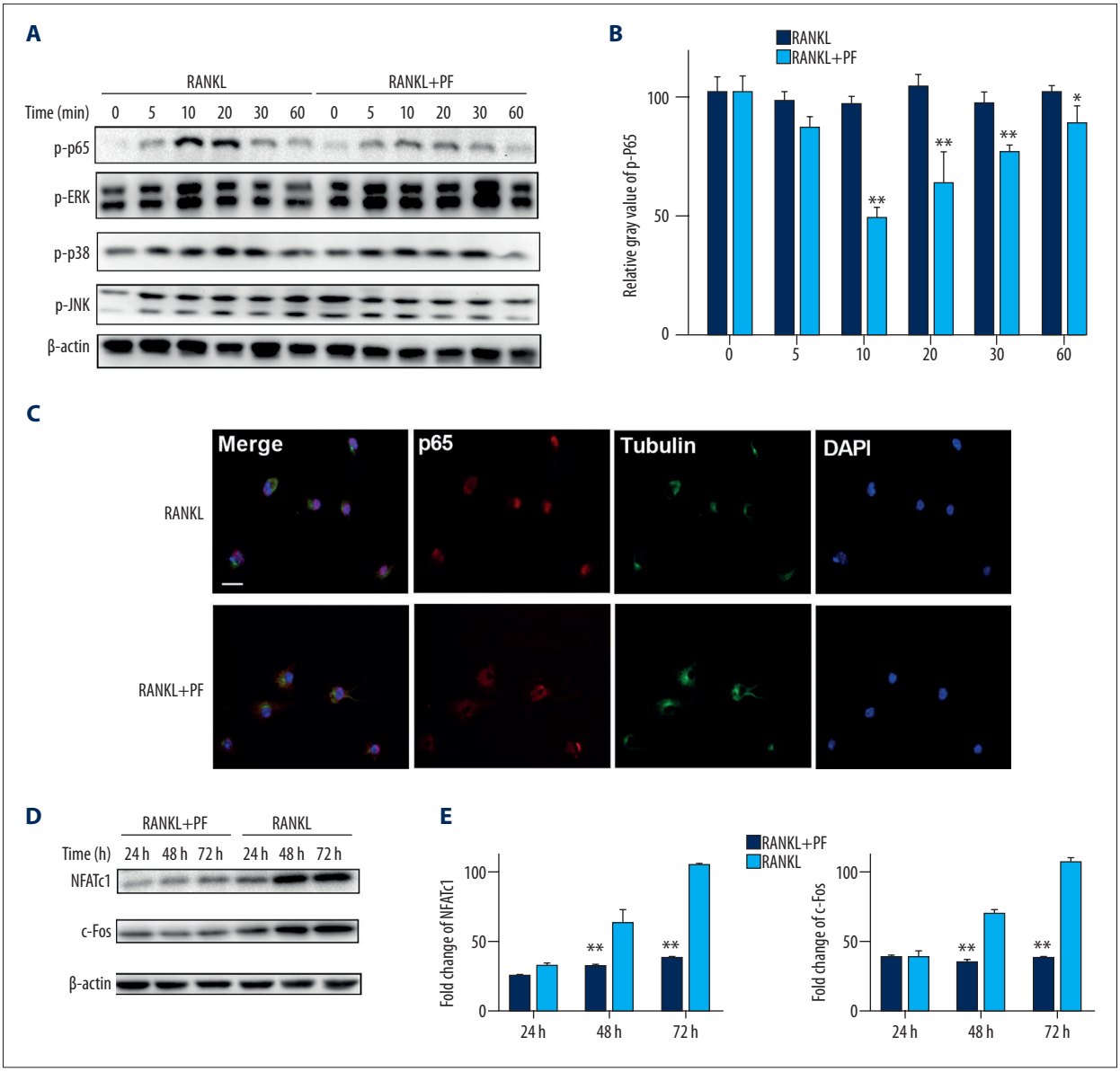

Figure 2. Paeoniflorin (PF) down-regulates receptor activator of nuclear factor-κB ligand (RANKL)-induced nuclear factor kappa B (NF-κB) activation and key osteoclast protein expression. (**A**) Bone marrow macrophages (BMMs) were incubated with or without 100 μmol/L PF for 1 h, followed by RANKL (100 ng/mL) stimulation for the indicated times. Cells were lysed for Western blotting. Downstream proteins induced by RANKL were detected (p-P65, p-P38, p-ERK, and p-JNK). All protein bands are from the same gel; however, they are noncontiguous. β-actin was used as housekeeping proteins. (**B**) Grey values of phosphorylated-p65 were measured using Image J software. The *t* test was used to determine significance of the results. (**C**) BMM cells were plated at a density of 1×10^4 cells in 6-well plates and treated with PF for 1 h, followed by stimulation with RANKL (100 ng/mL) for 15 min. The localization of p65 was visualized using immunofluorescence analysis. (**D**) BMM cells were stimulated by 100 ng/mL RANKL with or without 100 μmol/L PF for 1, 2, or 3 days. Cells were then lysed for blotting with antibodies against NFATc1, c-Fos, and actin. (F) Grey values were measured using Image J software. All experiments were repeated 3 times. * p<0.05, ** p<0.01. scale bar=20 μm.

PF inhibits particle-induced osteolysis and osteoclast formation *in vivo*

The mouse calvarial osteolysis model is frequently used in simulating particle-induced osteolytic disease. We utilized a cobalt-chromium-molybdenum (CoCrMo) particle-induced mouse calvarial osteolysis model to directly evaluate the effects of PF against localized particle-induced osteolysis. The CoCrMo particles had an average diameter of 100 nm (Figure 4B), which was reported to be clinically relevant [28]. We found

Indexed in: [Current Contents/Clinical Medicine] [SCI Expanded] [ISI Alerting System] [ISI Journals Master List] [Index Medicus/MEDLINE] [EMBASE/Excerpta Medica] [Chemical Abstracts/CAS]

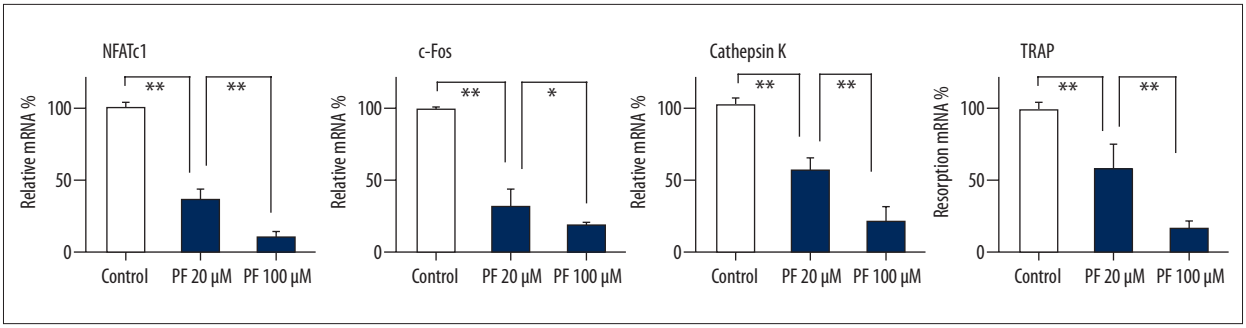

Figure 3. Paeoniflorin (PF) inhibits receptor activator of nuclear factor-kB ligand (RANKL)-induced osteoclast-gene expression. Bone marrow macrophages (BMMs) were incubated with RANKL (50 ng/mL) and murine colony stimulating factor (M-CSF) (30 mg/mL), as well as PF (20 μM and 100 μM), for 24 h. Osteoclast-specific genes (*NFATc1, c-Fos, cathepsin K,* and *TRAP*) were analyzed by realtime-PCR. β-*Actin* was used as the housekeeping gene. The experiment was repeated thrice. One-way ANOVA and Student-Newman-Keuls (SNK) tests were performed to measure significance between each group. * p<0.05, ** p<0.01

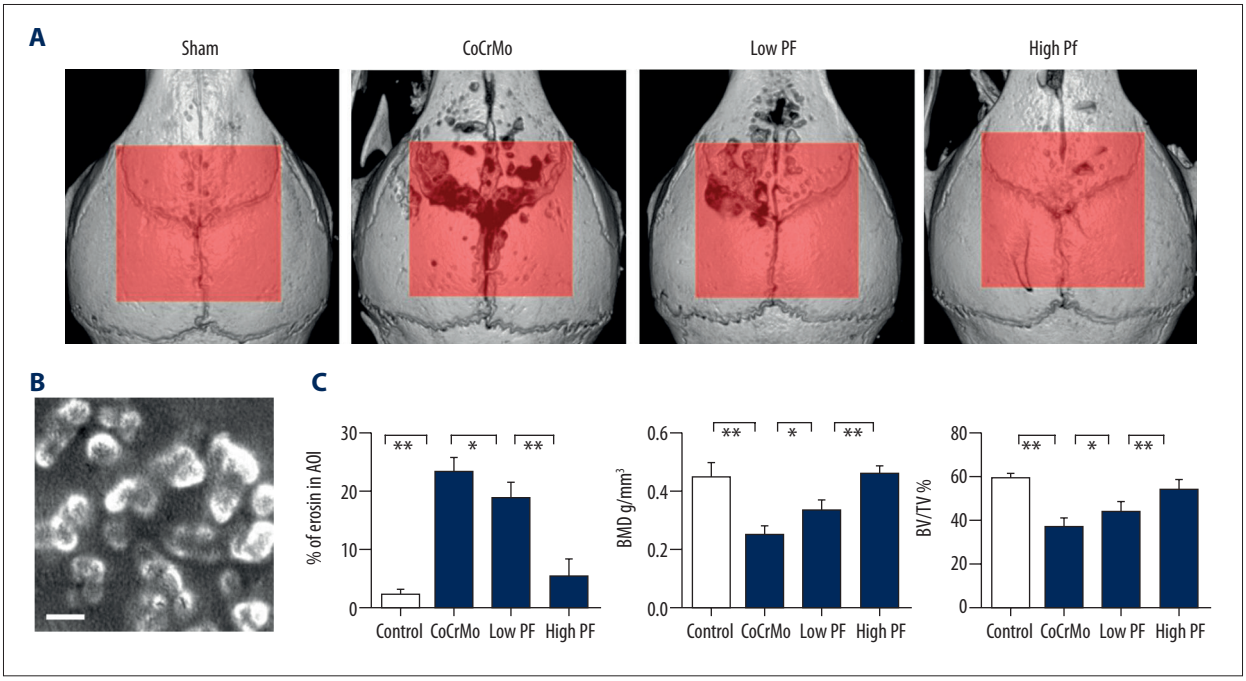

Figure 4. Paeoniflorin (PF) inhibited CoCrMo-induced bone destruction *in vivo* in a murine calvarial osteolysis model. Five C57BL mice per group including: shame operation group; CoCrMo alloy particles; Low PF (20 mg/kg/day); High PF (100 mg/kg/day). All mice were sacrificed at Day 7 after the operation. (**A**) Representative images of micro-computerized tomography (μ-CT) scans. (**B**) Representative SEM images of CoCrMo alloy particles; Bar=100 nm. (**C**) Percentage of erosion area in the AOI was measured via Image Pro Plus 6.0. Bone mineral density (BMD) and the bone volume to tissue volume (BV/TV) ratio was measured by the Micro-CT system; CoCrMo, cobalt-chromium-molybdenum; One-way ANOVA was used to determine significances of the results. Student-Newman-Keuls (SNK) test was performed to measure significances between each group. Area of interest (AOI) a square with the center falling in the middle of the coronal suture. * p<0.05, ** p<0.01

that cranium osteolysis was much more extensive in CoCrMo-treated mice than in control mice, as shown by μ-CT 3D reconstruction (Figure 4A). PF treatment significantly attenuated osteolysis and increased bone volume in a dose-dependent manner. Moreover, bone mineral density (BMD) and bone volume to tissue volume ratio (BT/TV) showed that PF treatment significantly preserved bone volume (Figure 4C).

Hematoxylin-eosin staining showed that CoCrMo particles lead to severe osteolysis and infiltration of inflammatory cell tissue. The results confirmed that PF inhibited bone loss and CoCrMo particle-induced inflammatory response (Figure 5A). In addition, there were fewer inflammatory cells, such as lymphocytes and macrophages, in the PF-treated mice than in mice treated with CoCrMo particles only. Consistent with the

Indexed in: [Current Contents/Clinical Medicine] [SCI Expanded] [ISI Alerting System] [ISI Journals Master List] [Index Medicus/MEDLINE] [EMBASE/Excerpta Medica] [Chemical Abstracts/CAS]

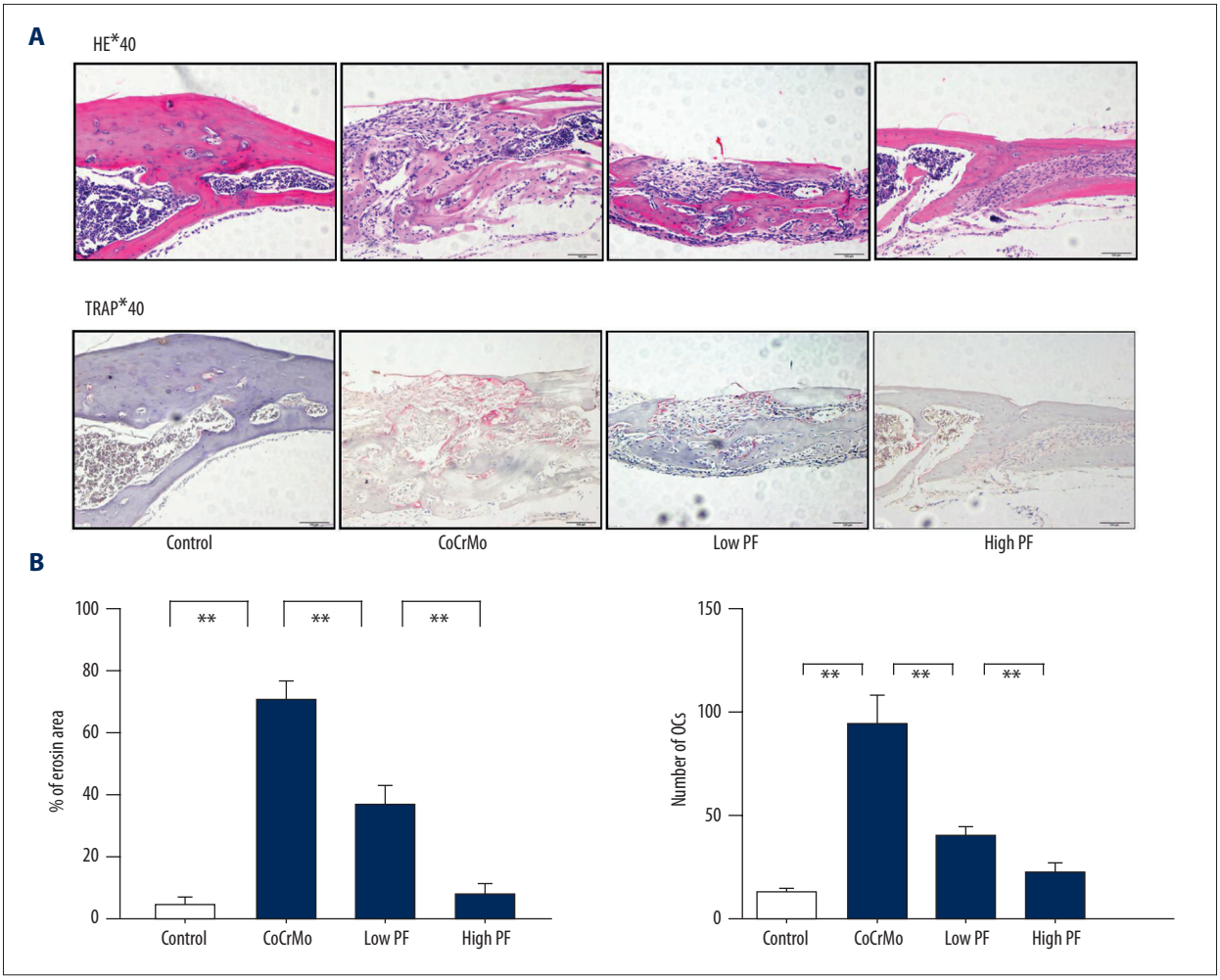

Figure 5. Paeoniflorin (PF) inhibits bone destruction and the number of tartrate-resistant acid phosphatase (TRAP)-positive osteoclasts, as shown by histological staining of calvaria sections. (**A**) Treatment with PF led to less bone erosion and inflammatory tissue in hematoxylin and eosin (HE)-stained slices. TRAP staining showed fewer osteoclasts in the PF-treated groups. High-dose treatment showed more inhibiting effect than low dose group. (**B**) Histomorphometric analysis of the erosion area (percentage of infiltrated fibrotic area against total tissue area) was performed. The number of osteoclasts in each slice was determined. One-way ANOVA and Student-Newman-Keuls (SNK) tests were performed to measure significance between each group. CoCrMo, cobalt-chromium-molybdenum; * p<0.05, ** p<0.01, scale bar=100 μm

micro-CT results, histomorphometric analysis demonstrated that PF significantly reduced the bone erosion induced by the CoCrMo particles (Figure 5B).

In TRAP staining, CoCrMo particles significantly increased the number of TRAP (+) osteoclasts on the surfaces of craniums (Figure 5B). PF treatment abolished the increase in osteoclast number caused by CoCrMo particles. Collectively, these results indicate that PF primarily disrupts osteoclast formation and bone resorption *in vivo*, thus suggesting that PF may be an effective anti-resorptive agent for the treatment of particle-induced bone destruction.

Discussion

In this study, paeoniflorin, which was widely used as an inflammation mediator previously, showed the capacity of attenuating RANKL-induced osteoclastogenesis as an NF-κB inhibitor in a dose-related manner, and we found an inhibiting effect of PF in particle-induced osteolysis *in vivo*.

Periprosthetic osteolysis and subsequent aseptic loosening remain the most common complications limiting the long-term durability of arthroplasty [29]. The joint revision arthroplasty operations lead to enormous medical expenses and significant surgery difficulties. Extensive efforts have been made to improve the implant design and biomaterials to avoid implant

Indexed in: [Current Contents/Clinical Medicine] [SCI Expanded] [ISI Alerting System] [ISI Journals Master List] [Index Medicus/MEDLINE] [EMBASE/Excerpta Medica] [Chemical Abstracts/CAS]

failure. However, all approaches are unable to eliminate particle generation from bearing surfaces, followed by a cascade of adverse biological reactions leading to periprosthetic osteolysis and the failure of THA. Even though the exact mechanism of aseptic loosening is unknown, particle-induced persistent inflammation, osteoclast formation, and the consequent bone resorption are known to be primary events in aseptic loosening [30,31].

PF is widely used in treatment of inflammatory disease and neurological system disease [32,33], but its pharmacological effects in the skeletal system has been seldom reported, especially in osteolysis diseases such as periprosthetic osteolysis. In the present study, we demonstrated that PF dose-dependently inhibited RANKL-induced osteoclast formation in BMMs. In addition, according to the osteo assay plate, PF also impaired resorption activity *in vitro*. To confirm the mechanisms of PF-associated impairment of osteoclast formation, we measured downstream proteins of RANKL/RANK pathway by Western blot. PF treatment inhibited phosphorylation of NF-κB but not MAPK (p38, ERK, and JNK) proteins. Moreover, inhibition of NF-κB p65 nuclear translocation in the PF-treated group was observed by immunofluorescent microscopy, indicating that PF exerted its inhibitory actions through NF-κB signaling rather than by MAPK signaling.

NFATc1 and c-Fos, which play essential roles in RANKL-induced osteoclastogenesis [24,34], are 2 critical transcriptional factors of the NF-κB and MAPK pathways [22]. Here, we showed that PF inhibited NFATc1 and c-Fos transcriptional activity and expression at both protein and mRNA levels. NFATc1 regulates the expression of genes associated with osteoclast differentiation and function, such as the *TRAP*, *cathepsin K*, *MMP9,* and *c-Src* genes. In this study, we also examined the expression of NFATc1-regulated genes, such as *TRAP*, and *cathepsin K* [35–38]. We found that they were also down-regulated by PF, suggesting that PF affects not only the expression of NFATc1, but also its downstream genes expression.

In an *in vivo* experiment, we used a murine calvarial osteolysis model with CoCrMo particles to determine if PF was effective on osteolytic disease. Micro-CT results indicated that PF treatment via intraperitoneal injection dose-dependently inhibited CoCrMo particle-induced calvarial osteolysis in mice, without any fatal complications. Histological analyses showed that CoCrMo particles significantly induced osteoclast formation *in vivo* and led to bone erosion. PF treatment remarkably impaired CoCrMo-associated osteoclast formation and preserved bone volume.

In this study we revealed that PF inhibited osteoclast formation *in vitro* and particle-induced osteolysis *in vivo*, but there are several limits to our research. We revealed that PF inhibited the activation of NF-κB pathway, but the exact mechanism needs further investigation. *In vivo* experiments using higher concentrations of PF are needed before the best dose can be confirmed.

In conclusion, the results of our work revealed that paeoniflorin exerts inhibitory effects on osteoclast formation as an NF-κB inhibitor. Although many of these inhibitors suppress osteoclastogenesis and bone resorption, some NF-κB inhibitors show severe adverse effects (e.g., triptolide shows hepatotoxicity and alimentary system lesions) [39,40]. Thus, new drugs for osteolysis disease, such as periprosthetic osteolysis, are still needed. Therefore, our study of PF suggests a new pharmacological treatment of osteolysis diseases.

Conclusions

In this research we found that paeoniflorin inhibits osteoclast formation *in vitro* and particle-induced osteolysis *in vivo*. In further experiments, we investigate the mechanism of the PF's protective effect. The results suggest that PF affects osteoclast formation and osteolysis as an NF-κB inhibitor. This work suggests that PF is a potential treatment for bone-construction disease.

Acknowledgements

None.

References:

1. Bedard NA, Pugely AJ, McHugh MA et al: Big data and total hip arthroplasty: How do large databases compare. J Arthroplasty, 2018; 33(1): 41–45.e3
2. Wang CT, Lin YT, Chiang BL et al: Over-expression of receptor activator of nuclear factor-kappaB ligand (RANKL), inflammatory cytokines, and chemokines in periprosthetic osteolysis of loosened total hip arthroplasty. Biomaterials, 2010; 31: 77–82
3. Jonitz-Heincke A, Lochner K, Schulze C et al: Contribution of human osteoblasts and macrophages to bone matrix degradation and proinflammatory cytokine release after exposure to abrasive endoprosthetic wear particles. Mol Med Rep, 2016; 14: 1491–500
4. Goodman SB, Ma T, Chiu R et al: Effects of orthopaedic wear particles on osteoprogenitor cells. Biomaterials, 2006; 27: 6096–101
5. Stea S, Visentin M, Granchi D et al: Cytokines and osteolysis around total hip prostheses. Cytokine, 2000; 12: 1575–79
6. Merkel KD, Erdmann JM, McHugh KP et al: Tumor necrosis factor-alpha mediates orthopedic implant osteolysis. Am J Pathol, 1999; 154: 203–10
7. Zaidi M, Troen B, Moonga BS, Abe E: Cathepsin K, osteoclastic resorption, and osteoporosis therapy. J Bone Miner Res, 2001; 16: 1747–49
8. Zhang J, Dou W, Zhang E et al: Paeoniflorin abrogates DSS-induced colitis via a TLR4-dependent pathway. Am J Physiol Gastrointest Liver Physiol, 2014; 306: G27–36

Indexed in: [Current Contents/Clinical Medicine] [SCI Expanded] [ISI Alerting System] [ISI Journals Master List] [Index Medicus/MEDLINE] [EMBASE/Excerpta Medica] [Chemical Abstracts/CAS]

9. Zheng M, Liu C, Fan Y et al: Neuroprotection by paeoniflorin in the MPTP mouse model of Parkinson's disease. Neuropharmacology, 2017; 116: 412–20
10. Zhang Y, Wang LL, Wu Y et al: Paeoniflorin attenuates hippocampal damage in a rat model of vascular dementia. Exp Ther Med, 2016; 12: 3729–34
11. Zhou H, Bian D, Jiao X et al: Paeoniflorin protects against lipopolysaccharide-induced acute lung injury in mice by alleviating inflammatory cell infiltration and microvascular permeability. Inflamm Res, 2011; 60: 981–90
12. Guo RB, Wang GF, Zhao AP et al: Paeoniflorin protects against ischemia-induced brain damages in rats via inhibiting MAPKs/NF-κB-mediated inflammatory responses. PLoS One, 2012; 7: e49701
13. Suska F, Gretzer C, Esposito M et al: *In vivo* cytokine secretion and NF-kappaB activation around titanium and copper implants. Biomaterials, 2005; 26: 519–27
14. Yamanaka Y, Karuppaiah K, Abu-Amer Y: Polyubiquitination events mediate polymethylmethacrylate (PMMA) particle activation of NF-kappaB pathway. J Biol Chem, 2011; 286: 23735–41
15. Zhao S, Yan L, Li X et al: Notoginsenoside R1 suppresses wear particle-induced osteolysis and RANKL mediated osteoclastogenesis *in vivo* and *in vitro*. Int Immunopharmacol, 2017; 47: 118–25
16. Weischenfeldt J, Porse B: Bone Marrow-Derived Macrophages (BMM): Isolation and applications. CSH Protoc, 2008; 2008: pdb.prot5080
17. Sawyer A, Lott P, Titrud J, McDonald J: Quantification of tartrate resistant acid phosphatase distribution in mouse tibiae using image analysis. Biotech Histochem, 2003; 78: 271–78
18. Shao H, Shen J, Wang M et al: Icariin protects against titanium particle-induced osteolysis and inflammatory response in a mouse calvarial model. Biomaterials, 2015; 60: 92–99
19. Darnay BG, Haridas V, Ni J et al: Characterization of the intracellular domain of receptor activator of NF-kappaB (RANK). Interaction with tumor necrosis factor receptor-associated factors and activation of NF-kappab and c-Jun N-terminal kinase. J Biol Chem, 1998; 273: 20551–55
20. Ru JY, Xu HD, Shi D et al: Blockade of NF-κB and MAPK pathways by ulinastatin attenuates wear particle-stimulated osteoclast differentiation *in vitro* and *in vivo*. Biosci Rep, 2016; 36(5): pii: e00399
21. Chaweewannakorn W, Ariyoshi W, Okinaga T et al: Ameloblastin and enamelin prevent osteoclast formation by suppressing RANKL expression via MAPK signaling pathway. Biochem Biophys Res Commun, 2017; 485: 621–26
22. Yamashita T, Yao Z, Li F et al: NF-kappaB p50 and p52 regulate receptor activator of NF-kappaB ligand (RANKL) and tumor necrosis factor-induced osteoclast precursor differentiation by activating c-Fos and NFATc1. J Biol Chem, 2007; 282: 18245–53
23. Huang H, Chang EJ, Ryu J et al: Induction of c-Fos and NFATc1 during RANKL-stimulated osteoclast differentiation is mediated by the p38 signaling pathway. Biochem Biophys Res Commun, 2006; 351: 99–105
24. Takayanagi H, Kim S, Koga T et al: Induction and activation of the transcription factor NFATc1 (NFAT2) integrate RANKL signaling in terminal differentiation of osteoclasts. Dev Cell, 2002; 3: 889–901
25. Yasui T, Hirose J, Tsutsumi S et al: Epigenetic regulation of osteoclast differentiation: possible involvement of Jmjd3 in the histone demethylation of NFATc1. J Bone Miner Res, 2011; 26: 2665–71
26. Kim K, Lee J, Kim JH et al: Protein inhibitor of activated STAT 3 modulates osteoclastogenesis by down-regulation of NFATc1 and osteoclast-associated receptor. J Immunol, 2007; 178: 5588–94
27. Ikeda F, Nishimura R, Matsubara T et al: Critical roles of c-Jun signaling in regulation of NFAT family and RANKL-regulated osteoclast differentiation. J Clin Invest, 2004; 114: 475–84
28. Kovochich M, Fung ES, Donovan E et al: Characterization of wear debris from metal-on-metal hip implants during normal wear versus edge-loading conditions. J Biomed Mater Res B Appl Biomater, 2017 [Epub ahead of print]
29. Dahlstrand H, Stark A, Wick MC et al: Comparison of metal ion concentrations and implant survival after total hip arthroplasty with metal-on-metal versus metal-on-polyethylene articulations. Acta Orthop, 2017; 88(5): 490–95
30. Patntirapong S, Habibovic P, Hauschka PV: Effects of soluble cobalt and cobalt incorporated into calcium phosphate layers on osteoclast differentiation and activation. Biomaterials, 2009; 30: 548–55
31. Jämsen E, Kouri VP, Ainola M et al: Correlations between macrophage polarizing cytokines, inflammatory mediators, osteoclast activity, and toll-like receptors in tissues around aseptically loosened hip implants. J Biomed Mater Res A, 2017; 105: 454–63
32. Zheng YQ, Wei W, Zhu L, Liu JX: Effects and mechanisms of Paeoniflorin, a bioactive glucoside from paeony root, on adjuvant arthritis in rats. Inflamm Res, 2007; 56: 182–88
33. Chen A, Wang H, Zhang Y et al: Paeoniflorin exerts neuroprotective effects against glutamate-induced PC12 cellular cytotoxicity by inhibiting apoptosis. Int J Mol Med, 2017; 40(3): 825–33
34. Matsuo K, Owens JM, Tonko M et al: Fosl1 is a transcriptional target of c-Fos during osteoclast differentiation. Nat Genet, 2000; 24: 184–87
35. Matsumoto M, Kogawa M, Wada S et al: Essential role of p38 mitogen-activated protein kinase in cathepsin K gene expression during osteoclastogenesis through association of NFATc1 and PU.1. J Biol Chem, 2004; 279: 45969–79
36. Kim K, Kim JH, Lee J et al: Nuclear factor of activated T cells c1 induces osteoclast-associated receptor gene expression during tumor necrosis factor-related activation-induced cytokine-mediated osteoclastogenesis. J Biol Chem, 2005; 280: 35209–16
37. Sundaram K, Nishimura R, Senn J et al: RANK ligand signaling modulates the matrix metalloproteinase-9 gene expression during osteoclast differentiation. Exp Cell Res, 2007; 313: 168–78
38. Aliprantis AO, Ueki Y, Sulyanto R et al: NFATc1 in mice represses osteoprotegerin during osteoclastogenesis and dissociates systemic osteopenia from inflammation in cherubism. J Clin Invest, 2008; 118: 3775–89
39. Wang J, Jiang Z, Ji J et al: Gene expression profiling and pathway analysis of hepatotoxicity induced by triptolide in Wistar rats. Food Chem Toxicol, 2013; 58: 495–505
40. Li XJ, Jiang ZZ, Zhang LY: Triptolide: progress on research in pharmacodynamics and toxicology. J Ethnopharmacol, 2014; 155: 67–79

Indexed in: [Current Contents/Clinical Medicine] [SCI Expanded] [ISI Alerting System] [ISI Journals Master List] [Index Medicus/MEDLINE] [EMBASE/Excerpta Medica] [Chemical Abstracts/CAS]